Ab initio study of MoS_2 nanotube bundles

Matthieu Verstraete* and Jean-Christophe Charlier
Unité de Physico-Chimie et de Physique des Matériaux (PCPM), Research Center on Microscopic and Nanoscopic Materials and Electronic Devices (CERMIN), Université Catholique de Louvain, Place Croix du Sud, 1, B-1348 Louvain-la-Neuve, Belgium
(Received 10 March 2003; published 30 July 2003)

Recently, the synthesis of a new phase of $MoS_2I_{1/3}$ stoichiometry was reported [M. Remskar, A. Mrzel, Z. Skraba, A. Jesih, M. Ceh, J. Demšar, P. Stadelmann, F. Lévy, and D. Mihailovic, Science **292**, 479 (2001)]. Electron microscope images and diffraction data were interpreted to indicate bundles of sub-nanometer-diameter single-wall MoS_2 nanotubes. After experimental characterization, the structure was attributed to an assembly of ''armchair'' nanotubes with interstitial iodine. Using first-principles total-energy calculations, bundles of MoS_2 nanotubes with different topologies and stoichiometries are investigated. All of the systems are strongly metallic. Configurations with ''zigzag'' structures are found to be more stable energetically than the ''armchair'' ones, though all of the structures have similar stabilities. After relaxation, there remain several candidates which give a lattice parameter in relative agreement with experiment. Further, spin-polarized calculations indicate that a structure with armchair tubes iodine atoms in their center acquires a very large spontaneous magnetic moment of $12\mu_B$, while the other structures are nonmagnetic. Our *ab initio* calculations show that in most of the other structures, the tubes are very strongly bound together, and that the compounds should be considered as a crystal, rather than as a bundle of tubes in the habitual sense.

DOI: 10.1103/PhysRevB.68.045423 PACS number(s): 61.48.+c, 73.20.At, 73.63.−b

Unidimensional nanostructures, and in particular nanotube systems, have received a great deal of attention in the past decade. Many interesting properties are directly associated to the small dimensions and high anisotropy of these intriguing tubelike structures. Potential applications range from nanoelectronics to efficient field emission, and materials with exceptional mechanical strength.[1] Carbon nanotubes were the first to be synthesized in 1991.[2] Since then, several groups have demonstrated that the synthesis of nanotubes could be achieved with other layered compounds, such as hexagonal boron nitride (h-BN),[3–5] the family of layered structures of BC_3 and $B_xC_yN_z$ stoichiometry,[6,7] the metal dichalcogenide family and many others. The first such structure to be synthesized was a nanotube of the dichalcogenide family (i.e., WS_2, MoS_2) which consisted of alternating layers of metal and sulfur.[8–10] These multiwall nanotubes were produced by passing reactive gases such as H_2S over films of W or Mo in reducing atmospheres. During the reaction, cylindrical structures a few dozen nanometers in diameter and of micron length are formed. Metal dichalcogenide nanostructures have been used as very high aspect-ratio scanning microscope tips,[11] and also exhibit interesting lubricating properties.[12]

Recently, the synthesis of MoS_2 nanotube bundles with very small diameter tubes has been reported.[13] The nanotubes are homogeneous in size and the bundles contain iodine, which is used as a transport agent, in proportions 1 Mo for 2 S for 1/3 I. Transmission electron microscope (TEM) images reveal hexagonally packed tubes with 9.6Å between adjacent tube axes. The space group $P6_3$ (C_6^6) is compatible with electron-diffraction images of the bundles. A potential structural model in which the iodine is placed in high-symmetry interstitial positions between the tubes, was also suggested, and is illustrated in Fig. 1

The aim of the present paper is to compare the stability of different structural models for the bundles, using first-principles calculations, in the quest for lower-energy structures which remain coherent with experimental data. In the following section (I), we present the models studied, and the technical details of our simulation methods. Then in Sec. II we present results on the relative stability of the different phases. Section III contains the comparison of the relaxed structures. Follows Sec. IV with the analysis of the electronic structure of the most interesting phases, and of the unexpected magnetism found in one of the structures. Finally, we discuss the results more globally, compare them with experiment, and conclude in Sec. V.

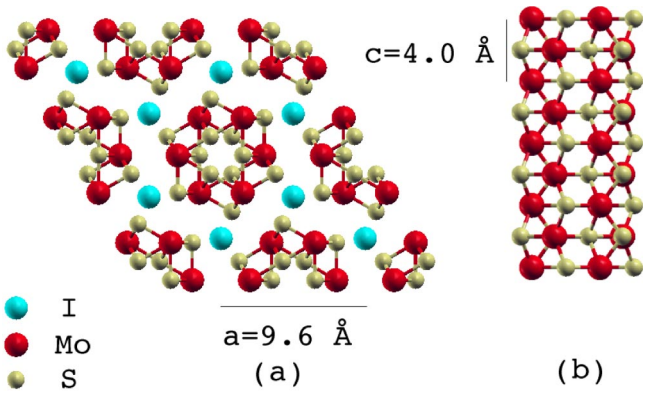

FIG. 1. (Color online) (a) Axis-on view of a periodic array of MoS_2 (3,3) armchair nanotubes, proposed in Ref. 13. An entire MoS_2 tube [Mo: large black (red in color version), S: small light gray (yellow) spheres] is present at the center, surrounded by six iodine atoms [I: dark gray (blue) spheres] and the edges of neighboring tubes within a 2×2 unit cell. An isolated MoS_2 armchair nanotube is extracted from this structure and depicted along its axis in (b).

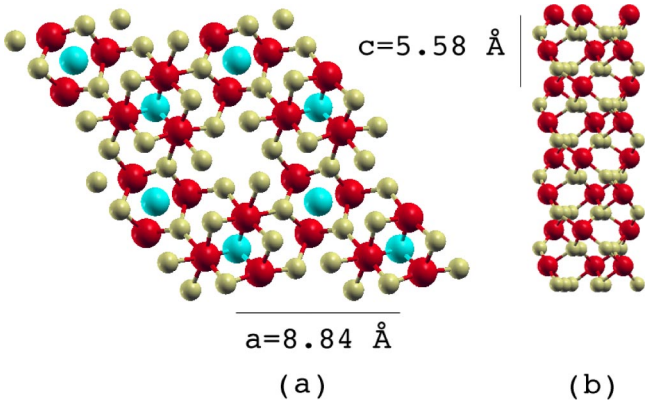

FIG. 2. (Color online) (a) View of a cross section of a periodic array of MoS_2 (3,0) zigzag nanotubes. (b) Side view of an isolated MoS_2 (3,0) armchair nanotubes extracted from the structure in (a).

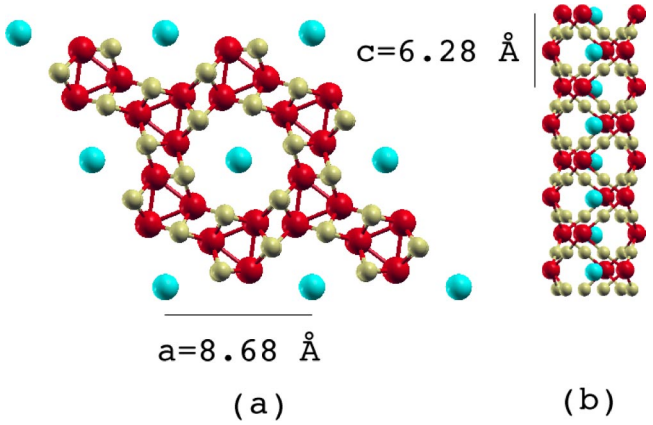

FIG. 3. (Color online) (a) View of a cross section of a periodic array of MoS_2 (3,0) zigzag tubes with iodine centered in the tube channels.

I. MODELS AND TECHNICAL DETAILS

A. Model systems for the MoS_2 NT bundles

We first consider the model as a hexagonal assembly of nanotubes of MoS_2. As shown in Ref. 14, a realistic topology of free-standing MoS_2 nanotubes is obtained similarly to that of carbon tubes, with half the carbons replaced by Mo, and the other half by two sulfur atoms: one inside and the other outside the average tube radius. The construction of fullerene-type systems by the same method allows the tubes to be capped while respecting the stoichiometry and topological conditions. Only large diameter tubes are predicted as stable, and indeed are observed experimentally. Making a bundle out of very small diameter tubes introduces very different constraints, as we will show in Sec. III.

Each nanotube topology can be characterized by two indices (n,m) giving both the helicity and the circumference $(n\vec{a}+m\vec{b})$ of the tube in the 2D basis $(\vec{a},\vec{b})$ of the layered MoS_2 structure. This defines two particular achiral symmetries, the ''armchair'' (n,n), and ''zigzag'' $(n,0)$ classes.[15] All other (n,m) nanotubes with $m \neq n$ are chiral.

The bundles we consider to begin with are assemblies of both zigzag (3,0) and armchair (3,3) configurations, with iodine first in interstitial then in ''in-tube'' positions along the tube axis. Sulfur being a lighter element than iodine or molybdenum, there is more uncertainty in its stoichiometry from the EDX experiments of Ref. 13. Two systems with less sulfur content are therefore also modeled, with stoichiometries Mo_3S_4 and Mo_6S_6. The unit cell contains 6 Mo, 2 I atoms, and from 6 to 12 S atoms.

For all configurations, the unit cell was kept hexagonal, and the space group of the system was always $P6_3$ (C_6^6), as suggested in Ref. 13. This is one constraint which could be loosened to search for other MoS_2 phases.

Based on the experimental stoichiometry of one iodine for three molybdenum, we suppose that the I atoms sit in high symmetry positions for $P6_3$. There are two possibilities. Either in (1/3, 2/3, 0) and (2/3, 1/3, 1/2), which we will call the interstitial positions, in reference to the initial structure proposed by Remskar *et al.* (see picture above). Or, the iodines can lie in (0,0,0) and (0,0,1/2), which we will call the ''in-tube'' or centered positions, as the iodine then lies in the channels of the tubes for the initial nanotube model. We emphasize that these are naming conventions, labeled with respect to the initial structure; the relaxation of these systems to their equilibrium positions in several cases completely changes the structure (though not the position of the I, which are fixed by symmetry).

Six model systems are thus investigated: armchair tubes with interstitial I (the model proposed in Ref. 13 Fig. 1 and Fig. 4), or with centered I (Fig. 5 and 6). Then zigzag tubes with interstitial (Fig. 2) or centered I (Fig. 3). Finally the two phases with less sulfur, Mo_3S_4 (Fig. 7) and Mo_6S_6 (Fig. 8), with centered iodine atoms. The equilibrium geometry of each of these phases is represented in Figs. 2–8.

B. Simulation methods and technical details

We have performed first-principles calculations of nanotube bundles using density functional theory (DFT) in the generalized-gradient approximation (GGA) of Perdew-Burke-Ernzerhoff,[16] as implemented in the ABINIT package.[17] The wave functions and the density are expanded on a plane-wave basis set. A kinetic-energy cutoff of 40 Ha is used for the plane waves. The interaction between valence

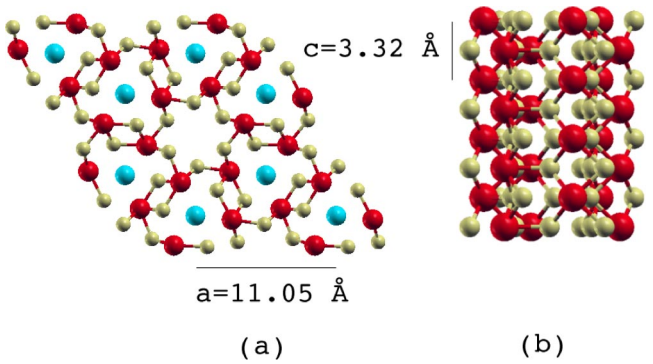

FIG. 4. (Color online) (a) View of a cross section of a periodic array of MoS_2 (3,3) armchair nanotubes. (b) Side view of an isolated MoS_2 (3,3) armchair nanotubes extracted from the structure in (a).

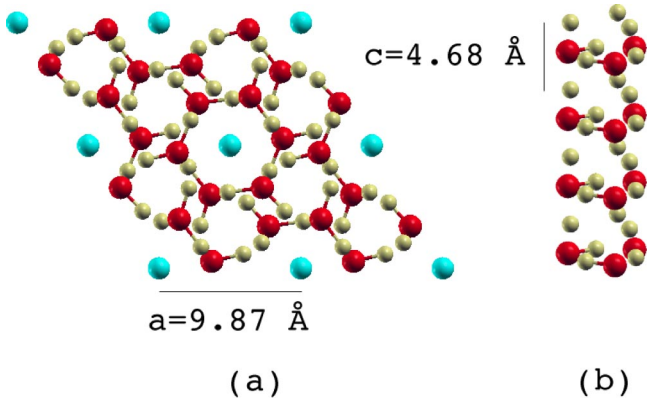

FIG. 5. (Color online) (a) View of a cross section of a periodic array of MoS_2 (3,3) armchair tubes with iodine centered in the tube channels. Spin-unpolarized calculation.

electrons and ionic cores is described using norm-conserving fully separable[18] pseudopotentials for I, Mo, and S of the Trouiller-Martins type.[19]

The atomic positions and lattice constants are allowed to relax completely using the Broyden algorithm,[20] until the forces were less than 5×10^{-4} eV/Å and the stresses less than 3×10^{-3} GPa. The one exception was the armchair centered system with spin polarization, whose forces and stresses saturated at a value less than 5×10^{-2} eV/Å and 5×10^{-2} GPa. The resulting displacements of atoms were smaller than 0.05 Å from step to step, and showed no drift, so the positions were considered converged.

The relaxation can be very lengthy due to soft modes of vibration, in which the tubes rotate around their axis. The total energies are converged to less than 2 meV per atom with 8 k-points sampling the irreducible wedge of the Brillouin zone. A cold-smearing broadening of 0.01 (Ha) was used to accelerate the convergence with respect to the number of kpoints.[21,22]

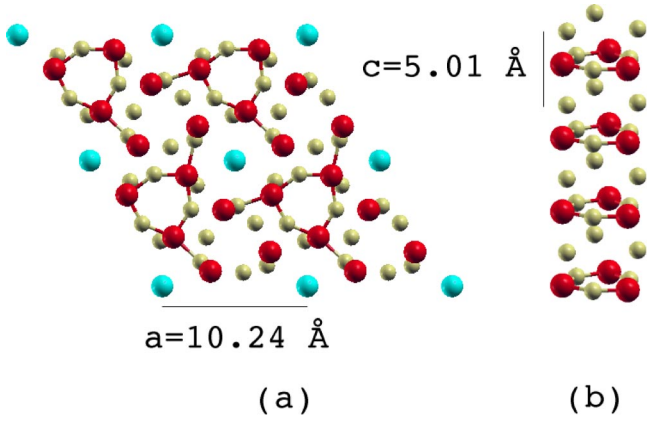

FIG. 6. (Color online) (a) View of a cross section of a periodic array of MoS_2 (3,3) armchair tubes with iodine centered in the tube channels, from a spin-polarized calculation. A permanent magnetic moment of $12\mu_B$ appears, and the structure relaxes to a significantly different minimum.

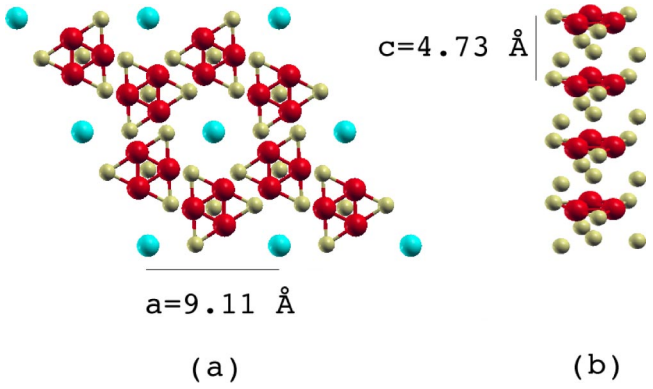

FIG. 7. (Color online) (a) View of a cross section of a system of Mo_3S_4 with iodine centered in the channels of the Nb_3S_4 type structure.

II. ENERGETICS

In this section we consider the relative stability of the different MoS_x systems. The four nanotube systems we consider have the same number of atoms of each atomic species, so the comparison of their relative stability is simple. However, in the case of the Mo_3S_4 and Mo_6S_6 systems, we have to choose reference systems in which the energy of one Mo, S, or I atom is well defined, in order to determine the relative binding energies. This choice will influence the final result: for example, choosing isolated atomic iodine as a reference will favor all systems where the iodine is bound. Choosing diatomic iodine will reduce this dependency, as I in I_2 has a lower energy.

The reference system of greatest interest in our case is planar hexagonal MoS_2. This is the bulk substance that is used in experimental synthesis, and is the most stable phase of MoS_2. The choice of *h*-MoS_2 gives the additional advantage of providing an external reference: instead of just considering the relative stabilities of the compounds, we can evaluate their ''absolute'' stability. Crystalline MoS_2 is naturally composed of graphitelike layers, bound together with Van der Waals interactions. The difference with h-MoS_2's binding energy represents the strain needed to roll up the

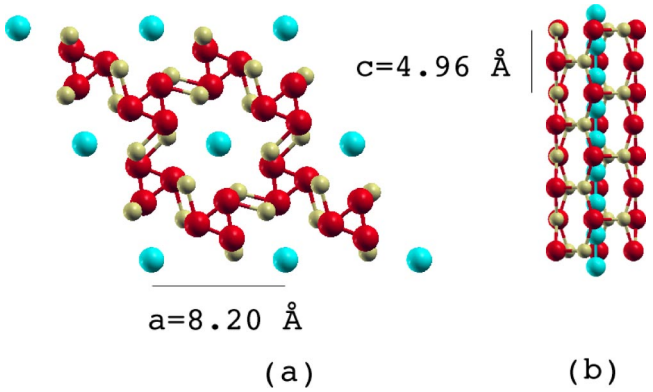

FIG. 8. (Color online) (a) View of a cross section of a system of Mo_6S_6 with iodine centered in the channels. The structure resembles a carbon nanotube, with half the atoms replaced by Mo and the other half by S.

TABLE I. Binding energies for different MoS_2 based systems. h-MoS_2 is the standard planar compound, the second column gives the value for the model from Ref. 13. zz interst: zigzag nanotubes with interstitial iodine. arm interst: armchair nanotubes with interstitial iodine. zz chan: zigzag tubes with iodine in the tube channels (centered). arm chan: armchair tubes with iodine in the tube channels (centered). arm chan spin: as arm chan, from a spin-polarized calculation. Mo_3S_4 and Mo_6S_6: see text and Figs. 7 and 8. Energies are calculated subtracting the energy of isolated atomic species.

Binding energy	h-MoS_2	model Ref. 13	zz interst	arm interst	zz chan	arm chan	arm chan spin	Mo_3S_4	Mo_6S_6
(eV/atom)	−4.16342	−2.15224	−3.29970	−3.12115	−3.18747	−2.71013	−3.02626	−2.70933	−2.81005

S-Mo-S layer, the interaction between tubes, and the binding energy of Mo and S with the iodine. For reference, a (10,0) carbon nanotube (with a diameter of around 8 Å) is estimated to have a strain energy of 0.1 eV/atom based on an LDA calculations.[23]

The binding energies presented in this section are calculated as follows. First a simple calculation is carried out for isolated atoms of Mo, S, and I. Then, the energy of these atoms is subtracted from, on the one hand, our phases of interest, and on the other hand a triple-layer of planar MoS_2. Finally, the energy is divided by the number of atoms in the system. This gives a uniform definition of the binding energy, whatever the stoichiometry, and allows us to compare the energy of the systems with the reference of h-MoS_2, and with the off-stoichiometry cases. Our results are summarized in Table I.

The results refer to spin unpolarized calculations. Adding spin polarization showed no magnetic moment in any system except the armchair tubes with centered iodine. In this case, quite surprisingly, a huge magnetic moment of $12\mu_B$ is found to be stable, and further relaxation of the geometric structure occurs (see below for the details of the geometrical and electronic effects, and a discussion of the calculation). As far as the energy is concerned (Table I column arm chan spin) it is naturally lowered with respect to the spin-unpolarized case for armchair tubes with I in the channels.

We can see from the table that *h*-MoS_2 remains substantially more stable than even the best phase by almost 1 (eV/atom). This is due to the strain energy which is added because of the strong curvature present in all these structures when compared to the planar sheet. The model from Ref. 13 is naturally not the most stable: it was proposed based on symmetry and volume considerations only, and had not been refined with energetic or steric considerations. The most stable phase is found to be zigzag (zz) tubes and interstitial iodine. The other nanotube-based structures, including the spin-polarized armchair case with centered I, come next, within less than 0.25 (eV/atom) from the zz interstitial value. Finally, the two off-stoichiometry models are some 0.2 (eV/atom) higher still. We thus have a set of phases with different atomic arrangements and similar binding energies.

The two main characteristics of our system, compared in particular to h-MoS_2 or to the large diameter free-standing tubes, are the bundle structures and the presence of iodine. On one hand, the iodine can bind with both molybdenum and sulfur, lowering the total energy. On the other hand, bonding with neighboring tubes expands each tube's diameter, reducing its curvature, and thus decreasing its internal strain. To separate the contributions of iodine binding and intertube binding, we first calculate the energy of a bundle without iodine. Then, a further calculation is carried out in which the tubes are separated by several Å. Is this way the two different contributions can be estimated.

This procedure is carried out for the most promising systems presented thus far (best binding energy and best geometry, respectively), viz. the zigzag interstitial and armchair centered spin-polarized systems. The zigzag interstitial system without iodine is found to be 5.66 (eV) higher in energy (Mo binding to the two I atoms). However, as there are fewer atoms in the system, the binding energy per atom is slightly more favorable: −3.35 (eV/atom) instead of −3.30 (eV/atom) with the iodine. When we further separate the tubes by about 7 Å, the system is then 11.7 (eV) [i.e., 0.65 (eV/atom)] higher in energy than the bundle with iodine. We emphasize that the tube was not allowed to relax to its equilibrium diameter, so the energy difference is only due to the binding between neighboring tubes. Since the tubes have precise Mo_1S_2 stoichiometry, we expect no dangling bonds, and negligible Van Der Waals interaction between tubes a this distance.

In the armchair centered case, extracting the iodine actually gives a slightly more bound system, by 0.51 (eV). This means the iodine is not binding to any of the species, and it even repels the surrounding atoms. This corresponds to the picture of Fig. 6(b) where the iodine appear bound to each other but to nothing else. As a result, the binding energy per atom is −3.39 (eV/atom), even better than in the zigzag interstitial case above. Separating the two tubes in each unit

TABLE II. *a* and *c* hexagonal lattice parameters (Å) and unit cell volumes (Å^3) for MoS_2 based compounds in zigzag and armchair configurations, with I in interstitial and centered positions, and in Mo_3S_4 and Mo_6S_6 configurations as explained in Table I. The first column gives the corresponding values used in the model in Ref. 13, estimated using TEM and x-ray diffraction data.

	model Ref. 13	zz interst	arm interst	zz chan	arm chan	arm chan spin	Mo_3S_4	Mo_6S_6
a	9.6	8.84	11.05	8.68	9.87	10.24	9.11	8.20
c	4.0	5.58	3.32	6.28	4.68	5.01	4.73	4.96
volume	214.04	235.81	253.41	274.4	264.8	304.9	228.2	193.9

TABLE III. Bond lengths (Å) in $(MoS_2)_6I_2$ compounds for nanotube-based configurations (armchair and zigzag tubes), with iodine in interstitial and centered positions. The last line shows S-Mo-S angles in degrees.

species-pair	zz interst	arm interst	zz center	arm center	arm center spin
Mo-Mo	3.06	3.32	2.83	3.59	4.15,4.36
Mo-S	2.32,2.37,2.40,2.46,2.53	2.44,2.45,2.55,2.60,2.91	2.33,2.36,2.41,2.46, 2.51,2.55	2.24,2.61,2.65,2.79	2.35,2.49,2.62,2.98
Mo-I	2.64	3.33	3.85	3.70	3.61
S-S	3.26,3.35,3.37,3.40	2.93,3.01,3.29,3.32	2.86,3.11,3.17,3.34, 3.38,3.45	2.71,2.78	2.84,2.92
S-I	2.96,3.33,3.42	3.09,3.87	3.61,3.69	3.27	3.31
I-I	5.58	3.32	3.14	2.34	2.44
$\alpha_{S\text{-}Mo\text{-}S}$	87,91.6,93,174	69,72,86,84, 133,136,146	85,93,73,123,147	90,94,101,124	79,101,103,111

cell by 6 Å raises the energy by 0.71 (eV/atom). This value is comparable to that obtained for the manifestly bound zigzag interstitial case, which implies that the tubes are still strongly bound together: although the distance between atoms in separate tubes of the relaxed structure is larger, the clusters of Mo_3S_6 are interleaved, and still interact with neighboring tubes.

III. GEOMETRY AND RELAXED STRUCTURES

The relaxed atomic structure of the solid state phases is a very important criterion to extract interesting models from the chaff. In the GGA, most lattice parameters can be calculated to within a few percent of experiment. Exceptions are systems with long-range or Van der Waals forces, which are not accounted for in standard density functionals, or highly ionic systems, in which the pseudopotential approximation could become apparent. Our system could fall into the first of these categories, as h-MoS_2 displays VdW interactions between its layers. Nevertheless, we expect at least reasonable agreement with the experimental values of $a \simeq 9.6$ Å and $c \simeq 4.0$ Å

A. Lattice parameters

In this section we present the relaxed lattice parameters and atomic positions for the six phases described above. The lattice constants and unit cell volumes are summarized in Table II.

The two zigzag configurations and Mo_6S_6 have lattice parameters a smaller than the experimental value; armchair tubes and Mo_3S_4 give a larger a. The c lattice parameter is systematically too large, except for the armchair interstitial case. The specific case of the armchair configuration with spin-polarization presents the largest volume. This is probably the effect of same-spin electron repulsion: the total magnetic moment is large, and the majority spin state is very populated. Mo_6S_6 is the only system with a small unit cell volume. This is natural, as the number of sulfur atoms is much smaller than in the other models (6 instead of 12). Similarly, the volume of Mo_3S_4 is lower than that of the other systems. Globally, the overestimation of the volume is an effect of the GGA approximation which usually overestimates distances (whereas LDA underestimates them).

B. Bond lengths and angles

The types of bonding vary widely between the different models. The bond lengths and the angles between bonds in the different relaxed structures are collected in Tables III and IV. Values are also given for the initial model in Ref. 13, along with the VdW and covalent radii, and the bonds in h-MoS_2. The fact that GGA usually overestimates distances must be kept in mind when analyzing the bond lengths.

Covalent bonding appears between Mo and S in all cases, but the initial nanotube structures are completely distorted. Bonding appears between tubes and forms a three-dimensional (3D) lattice in the zigzag cases, the armchair

TABLE IV. Bond lengths (Å) in $(MoS_x)_6I_2$ compounds, and the model from Ref. 13. Column 5 shows the Van der Waals radii, column 6 the covalent radii, and column 7 the bond lengths in crystalline MoS_2. The last line shows S-Mo-S angles in degrees.

species-pair	Mo_3S_4	Mo_6S_6	Model of Ref. 13	VdW radii	covalent radii	h-MoS_2
Mo-Mo	2.46	2.30	3.51		2.60	3.15
Mo-S	2.43,2.50,2.76,2.86	2.51,2.63,2.68	2.46,2.49,3.36		2.32	2.35
Mo-I	4.23	3.75	3.37		2.63	
S-S	3.00,3.49	3.26	2.49	3.6	2.04	2.98, 3.66
S-I	3.49	3.42	2.79	3.78	2.35	
I-I	2.37	2.48	4.00	3.96	2.66	
$\alpha_{S\text{-}Mo\text{-}S}$	82,91,180	79,172,127	60,90,108,122,146			101

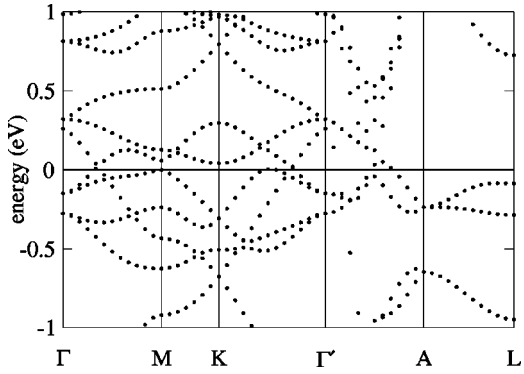

FIG. 9. Band structure of a bundle of armchair MoS_2 nanotubes with interstitial I.

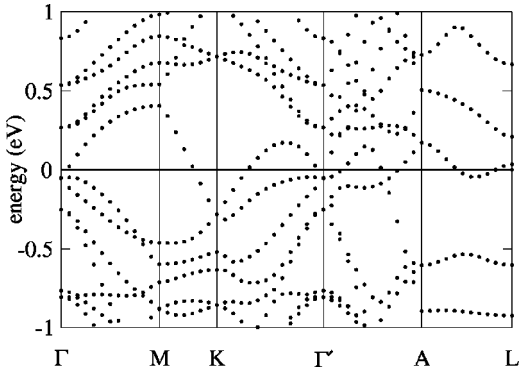

FIG. 10. Band structure of a bundle of zigzag MoS_2 nanotubes with interstitial I.

interstitial, and in Mo_6S_6. In the armchair interstitial structure, the intertube Mo-S bond is 2.60 Å (slightly longer than the 2.39 Å intratube distance), but in the zigzag case there are Mo-S intertube bonds of only 2.32 Å, and the intratube bonds are either 2.27, 2.33, or 2.44 Å. The systems are thus very strongly bound and the structures are not so much a bundle of loosely held tubes as a kind of zeolite structure with nanochannels at the center of the ''tubes.'' Iodine in the centered position binds to itself, whereas there are many I-Mo bonds in the interstitial structures, and the whole structure is tightly bound.

The Mo_3S_4 structure is interesting, consisting in small clusters of three Mo and three S atoms, capped with an S atom above and below. The clusters are separated from each other by roughly 2.9 Å, and are stacked in alternating planes at the (1/3,2/3,0) and (2/3,1/3,1/2) positions of the hexagonal unit cell.

The armchair centered structure also shows an interesting evolution: from the initial nanotube structure, the spin-unpolarized relaxation gives an exploded structure with S-Mo-S units. The further spin-polarized calculation reconstitutes clusters, as in Mo_3S_4, which are hexagons of Mo_3S_6, in alternating layers once again, and separated by 2.7 Å. The hexagons overlap each other with sulfur atoms, but can be seen as interlaced tubelike structures. With respect to these new tubes, whose axes are now at (2/3,1/3) or (1/3,2/3), the iodine is once again interstitial [though still at its original (0,0,0) position]. The tube packing is no longer simply hexagonal: the two tube positions alternate on a hexagon around the channels of iodine. The configuration is shown in part (b) of Fig. 6.

The coordination of Mo can vary strongly in its different oxidation states, so the wide variety of S-Mo-S angles should not come as a surprise. Only the armchair centered case (with or without spin polarization) presents angles similar to those in *h*-MoS_2, but the trimers of S-Mo-S involved are not strictly perpendicular to the tube axis.

Our findings can be compared with the isolated MoS_2 nanotube calculations of Seifert *et al.*[14] who used a DFT-based *tight-binding* method: the tubes are found to be stable for large diameters (>20 Å), and their strain energy follows a $1/D^2$ law where D is the diameter of the tube. Extrapolating their calculations of strain energies, stand-alone (3,3) and (3,0) tubes should be highly unstable. Furthermore, according to the trend in Ref. 14, these isolated (3,m) tubes should have very small diameters ~ 5 Å.

The atoms which should correspond to individual nanotubes, cut out of the bundles, are shown in parts (b) of Figs. 2–8. The effective diameter of the ''tubes'' is found to be much larger: 8 Å for the zigzag and 8.5 Å for the armchair tubes. In the armchair centered structure, the effective diameter is 8.3 Å. Once the structure is allowed to spin polarize, the new tubes which form have a very small ~ 5 Å diameter, but a topology which is different from the original armchair.

IV. ELECTRONIC STRUCTURE AND MAGNETISM

A. Band structures

In Ref. 13 it is suggested that the tubes should be metallic. In order to check this, we calculate the band structures of the various bundle systems. All of the systems are metallic (contrarily to *h*-MoS_2 which is an insulator).

Figures 9 and 10 show the electronic band structure for the armchair and zigzag bundles, respectively, with iodine in the interstitial position. Both systems are also metallic along the tube axis (Γ-A line). This is consistent with calculations for isolated nanotubes,[14] where the band gap increases with the tube diameter, and is close to 0 for diameters around 9–10 Å. But both bundles are also metallic in the direction perpendicular to the tube axis. This is a further consequence of the strong bundle structure. In Fig. 11 the band structure for the armchair centered case is shown.

B. Magnetism

The entire set of systems was recalculated in spin-polarized DFT where two spin orientations are allowed. The exchange-correlation energy then depends on both spin-up and spin-down densities, or equivalently on the total electron density and on the magnetization density (see Ref. 16)

$$\xi(x)=\frac{n_{\uparrow}(x)-n_{\downarrow}(x)}{n(x)}. \tag{1}$$

Among the six systems, only the armchair centered case displays a net magnetic moment. This is very intriguing, as the different configurations can be very similar in stoichiometry

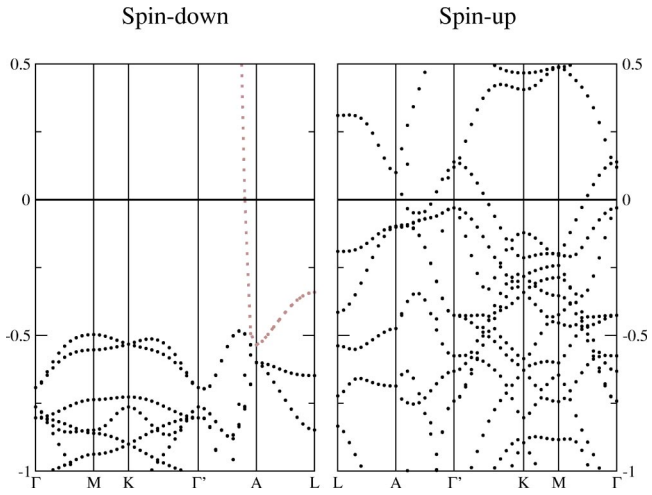

FIG. 11. Band structure of a bundle of armchair MoS_2 nanotubes with centered I.

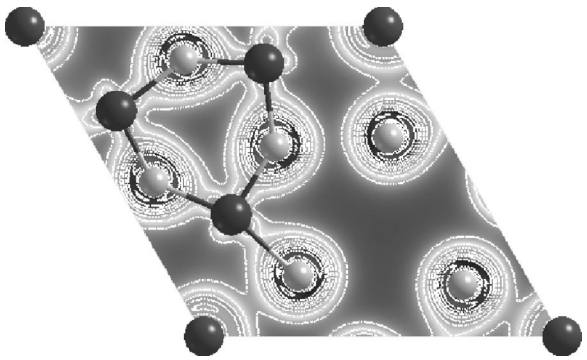

FIG. 12. Difference between spin-up and spin-down electron densities, slice of the unit cell of a bundle of armchair MoS_2 nanotubes with centered I. Spin-up density is dominant in spheres around the sulfur atoms. The isolines follow multiples of 0.01 (electrons/$Bohr^3$).

and/or geometry. A slice of the difference in spin-up and spin-down densities is shown in Fig. 12. The magnetization is localized around the sulfur atoms, in rough spheres, with the spins aligned parallel to each other. The initial spin-up spin-down symmetry must be broken in order for the system to converge to its physical minimum. This is done by starting from initial densities $n_\uparrow$ and $n_\downarrow$ which favor the up or down density on certain atoms. We also tested that the aligned configuration is the minimum of the energy when the starting density has antiparallel spins on the two inequivalent sulfur atoms. A simulation of the system without the iodine atoms also reveals a similar magnetic moment.

The zigzag tubes with centered I have a very similar structure in the *x*-*y* plane, and the molybdenum atoms are roughly in the same place. However, in the armchair case the sulfur are in the same plane as the Mo, whereas for the zigzag case they are in alternating planes halfway between the Mo. As a result, the zigzag structure has a smaller *a* lattice constant, and a larger *c*; the armchair configuration has to accommodate all the Mo and S atoms in the same plane, and thus becomes larger. In both cases there are sulfurs which bridge from one Mo atom to another, but in the armchair configuration there are also S atoms with only one close molybdenum.

V. DISCUSSION

The binding energies of all the phases are within an interval of 0.5 (eV/atom). In these conditions, one can envisage their coexistence, and the phase which will actually be synthesized will depend very strongly on the experimental conditions, on the catalysts used, and on the kinetics of the reaction. We now consider the experimental data and other criteria which can help us evaluate the different models, and propose new directions for research on these materials.

A. Formal valence and coordination

The natural valence states for S is $^-2$, and therefore a Mo which is $+4$ (as in MoS_2) satisfies the valence. Mo can adopt a number of different oxidation states, from $+2$ to $+5$ or even $+6$ with fluorine (in MoF_6). The presence of iodine in the lattice complicates the balance: the iodine can be in a $^-1$ or a neutral (0) state. In all the centered cases, the proximity of other iodine atoms and the greater distance from Mo and S make the 0 valence more realistic. This is also coherent with the binding energy of iodine in the armchair centered case (see below). In the interstitial cases, the iodine is much more closely bound to Mo or S, and is more probably I^-. Some of the Mo should become $+V$, but by symmetry all of the atoms are equivalent, so the formal valence state is a partial $+4.333$. In the case of Mo_3S_4I, the formal valence is satisfied for I^-, if the Mo are $+3$.

The $+3$ state should correspond to an octahedral coordination of the Mo, as explained in Ref. 24. In Mo_3S_4 and Mo_6S_6, the Mo are in clusters with three Mo, bridging S atoms, and additional capping S for Mo_3S_4. This follows remarkably well the distorsion of the lattice observed in Ref. 24, where three atom Mo clusters are also formed. The presence of Li, or iodine in our case, can change the average valence by adding or subtracting an electron, and favors metallic Mo-Mo bond formation.

Mo$+4$, as in MoS_2 should lead to Mo atoms at the center of trigonal prisms. Mo$+3$ or $+5$ is roughly octahedral once again, as in $MoCl_5$ and $MoCl_6$.[25] The only difference between the trigonal and octahedral shapes is the elongation of one axis. In the armchair interstitial system the environment is trigonal prismatic but is severely distorted. A seventh sulfur atom is present at 2.9 Å. For the armchair centered model, the Mo is in a distorted octahedral site, but two of the sulfurs are at 2.7 Å, and one apex is an iodine which is far away at 3.6 Å. This difference in coordination is suggested to play a key role in the magnetization which appears. The coordination of the sulfur is also particular in this system: there are S atoms with only one close Mo neighbor. The other systems always present S which is at least two-fold coordinated.

The zigzag interstitial system presents almost perfectly octahedral coordination for Mo, with one iodine neighbor: each S and each I is shared by three Mo atoms. The structure is strikingly similar to that of $MoCl_4$, which also creates

hexagons of Mo linked by (divalent) Cl atoms. In the zigzag centered model, the Mo is eightfold coordinated: three-atom Mo clusters form (as in Mo_3S_4 and Mo_6S_6), and the surrounding octahedron of sulfur is still present.

To sum up, the coordination of Mo is always octahedral-like, but in the armchair cases it is more severely distorted. Octahedral is the preferred coordination for Mo in clusters and solids; the trigonal coordination only appearing for exactly +IV valence, as in h-MoS_2. Perfect trigonal coordination never happens in our systems, either because of a fractional valence, or for sterical reasons.

B. Intertube binding

In the Mo_3S_4 and the armchair centered systems, there are loosely bound clusters of atoms. This is important, as Remskar *et al.*[13] report that by sonication they can separate ropes of very small numbers of tubes from the bulk bundles. It would be interesting to analyze the chemical composition of the rope (for example by electron energy loss spectroscopy) to see if it still contains iodine or if the dispersion succeeded in isolating just MoS_2 tubes. The tight covalent bonding between all atoms in the other models studied would seem to preclude this possibility. In carbon nanotube bundles, the intratube binding is very strong (similar to the in-plane graphite sp^2 bond), and the interaction between tubes is much weaker (Van der Waals). The dispersion of individual carbon tubes is thus fairly simple.

C. Iodine desorption

Experimentally, pumping over the MoS_2 bundles releases almost all of the iodine.[26] In the interstitial cases, the extraction of the iodine will be difficult, as the binding energy for the zigzag tubes is positive. However, the system is more stable in energy per atom in the final state. This is probably due to the ''frustrated'' valence of Mo described above. In the armchair centered configuration, the expulsion of iodine is almost certain: no binding occurs, and the iodine is probably already in a 0 valence state, so no charge transfer to the lattice is needed before I_2 can escape. The iodine only takes up space in the crystal, which explains why the system relaxes even further when the I is extracted. The binding energy per atom in the lattice is then more advantageous without iodine. As experiment demonstrates the presence of I in the lattice, it is probable that kinetic factors dominate, and I is incorporated into the lattice during its formation.

D. Iodine as an insertion component

Since the iodine in our systems is and insertion component, a natural way to change the lattice parameter is by adding or removing iodine. The quantity of iodine actually incorporated in the lattice will determine how bloated it is, and once the iodine is extracted a will return to its equilibrium value. Another possibility is the substitution of I for one of the S atoms. Iodine has a larger ionic radius, but only one valence electron to take from the system, instead of two for sulfur.

Iodine often substitutes for sulfur atoms in inorganic compounds. This effect could contribute to the residual iodine which is not desorbed. However, we have not studied the energy of substitution here, because of the stoichiometric amount of the iodine in the compound, and the manifest long range periodicity of the system. There is too much iodine for the atoms to be randomly substituted. It is more probable that they occupy a given optimal place in the lattice. Nevertheless, adding iodine substitution opens many additional routes to model building, which should also be considered.

E. Stoichiometry

Precise measurements of the stoichiometry of the bundles would bring precious evidence for further simulation work. As shown by Mo_3S_4, a similar lattice parameter and binding energy can be obtained with a sulfur-poor phase.

F. The effects of helicity

Hsu *et al.* reported the synthesis of MoS_2 nanotubes with a new method using MoS_2 powder instead of the MoO_3 (Ref. 27) used previously. This is similar to the process used by Remskar *et al.*,[13] and in both cases tubes grow perpendicular to the substrate. Hsu *et al.* argue that this type of perpendicular growth favors zigzag tubes, and they observe zigzag structures in the tubes they synthesize. The energetics suggest this is could be true: the zigzag tubes are more stable, with I centered or interstitial. However, the difference in binding energy is small, and the lattice geometries suggest the experimental phase is not one of the zigzag ones, as they both underestimate a (which should be overestimated, based on the considerations in Sec. III).

As the experimental tube spacing is intermediary between those we find for zigzag and armchair tubes, it is natural to think of intermediate-diameter tubes, with $(n,m)=(3,1)$, or (3,2) as possible candidates for models. The resulting structure will probably be distorted, as it is observed for (3,0) and (3,3) tubes, but the relative dimensions of the systems could be conserved. As the size of the repeated periodic cell increases dramatically for chiral tubes [i.e., 260 atoms for (3,1) and 380 atoms for (3,2) instead of 20, due to the tube chirality and the added iodine], these *ab initio* calculations would be lengthy, given the difficult relaxation and soft modes present. Further, we do not believe that this is a very promising path, for several reasons. For one, the high degree of crystallinity of the system would be blurred. With chiral nanotubes, diffraction spots are doubled according to the chiral angle of the tubes,[28,29] and the spots are rotated with respect to the tube axis. Also, the relative stacking of the tubes would have to be fixed, or even more disorder would be present in the system: in a bundle of tubes with intermediate helicities, there can be an offset, along the tube axis, between equivalent atoms of any two neighboring tubes, which adds additional (internal) degrees of freedom to the system.

The apparent uniformity of the bundles throughout the ''fur'' described in Ref. 13 is actually strikingly different from carbon nanotube bundles, which are never monohelical once they pass a certain size, and the individual tubes

also have a spread of diameters. This can be explained by a crystal structure like those we present in this article: 3D growth would create only one type of ''tube'' or crystal. All previous synthesis of MoS_2 nanotubes and fullerenes had yielded multilayer structures.[10,27]

G. Electronic structure

The metallicity of the bundles is something which should be easy to measure by scanning tunneling microscopy (STM). Further, scanning tunneling spectroscopy (STS) could differentiate between the proposed structural models based on their local densities of states. STM would also be an interesting complementary technique to study the atomic structure of the bundles. This will probably necessitate low-temperature STM experiments, for atomic resolution and for accurate STS measurements.

The unexpected magnetic results could be verified locally with magnetic force microscopy. One could presume the magnetic structure is erroneous, in particular the error could be due to the pseudopotential approach and the absence of dynamic interactions with the core electrons. However, in this case the error should be present in all of our very similar structural models. The fact that only one of the systems presents a magnetic moment, and that this moment is very stable with respect to geometric relaxation, magnetic perturbation, and the extraction of the iodine leads us to believe that the moment is a true physical characteristic of the atomic configuration. Nevertheless, we hope that this result in particular will be checked in the future using all-electron methods.

VI. CONCLUSIONS

In this article we present first-principles simulations of MoS_2 nanotube bundle systems. Starting from the model proposed in Ref. 13, based on experimental data, we explore a set of physically reasonable models with different stoichiometries and geometries, looking for the most probable candidate to explain experiment. Based on our present calculations, there is not enough experimental evidence to discern which of the phases has been truly synthesized. Several conclusions can nevertheless be reached.

First, the experimental model based on the armchair configuration with interstitial I can probably be infirmed, as such a structure gives too large lattice parameters, is less stable than the zigzag configuration, and gives a tightly bound 3D crystal. However, the closely related armchair centered model could be a realistic candidate.

Six different MoS_x+I phases have been studied, with relatively similar binding energies. Further experimental work will be needed to determine whether the phase in Ref. 13 is among them, and if some or all of the systems we have reviewed can be synthesized by changing the experimental conditions. Other MoS_2 phases can be generated by changing the symmetry or the stoichiometry even further. We believe the most representative examples have been covered here, i.e., those with the space group proposed from experiment, and which conserve the experimental stoichiometry for the heavier elements Mo and I, and S when possible. In each system, there is only one irreducible Mo atom, and two S atoms: all the other positions are deduced from the symmetry.

In the interstitial systems, the iodine is more tightly bound to the lattice. This is a first important test for experiment: can all of the iodine present in the bundles be extracted, or only a fraction, or none at all? Only the armchair centered and Mo_3S_4 systems present Van der Waals interactions in the plane perpendicular to the bundle axis. As such, the second important experimental criterion is the dispersion of small strands of the phase, which excludes the possibility of strong binding between the strands in the bundle.

We hope that the present study will stimulate more experimental work on these small-dimensional dichalcogenide systems, in order to provide evidence of their structure at the atomic level. This could be done using STM or MFM imaging, or EELS studies of the bundle stoichiometry. The catalytic mechanism of C_{60} still has to be clarified, and could shed light on the charge state of the different elements in the system.

ACKNOWLEDGMENTS

The authors wish to thank X. Rocquefelte and A. De Vita for very interesting and useful discussions, R. Seshadri for help checking the magnetism of different phases, and D. Mihailovic for in-depth discussions and access to recent developments on the experimental front. J.C.C. acknowledges the National Fund for Scientific Research (FNRS) of Belgium for financial support. This paper presents research results obtained thanks to the Belgian Program on Inter-university Attraction Poles (PAI5/1/1) entitled *Quantum Size Effects in Nanostructured Materials*, FRFC Project No. N2.4556.99*Simulations numériques et traitement des données*, and the Communauté Française through the Action de Recherche Concertée entitled *Interaction électron-vibration dans les nanostructures*. This work is carried out within the framework of the EU Human Potential - Research Training Network, project under Contract No. HPRN-CT-2000-00128.

*Electronic address: verstraete@pcpm.ucl.ac.be

[1] *Carbon Nanotubes*, edited by M. Dresselhaus, G. Dresselhaus, and P. Avouris, Vol. 80 of *Topics Appl. Phys.* (Springer-Verlag, Berlin, 2001).
[2] S. Ijima, Nature (London) **354**, 56 (1991).
[3] N. Chopra, R. Luyken, K. Cherrey, V. Crespi, M. Cohen, S. Louie, and A. Zettl, Science **269**, 966 (1995).
[4] A. Loiseau, F. Willaime, N. Demoncy, G. Hug, and H. Pascard, Phys. Rev. Lett. **76**, 4737 (1996).
[5] D. Golberg, Y. Bando, M. Eremets, K. Takemura, K. Kurashima, and H. Yusa, Appl. Phys. Lett. **69**, 2045 (1996).
[6] Z. Weng-Sieh, K. Cherrey, N.G. Chopra, X. Blase, Y. Miyamoto, A. Rubio, M.L. Cohen, S.G. Louie, A. Zettl, and R. Gronsky, Phys. Rev. B **51**, 11 229 (1995).
[7] K. Suenaga, C. Colliex, N. Demoncy, A. Loiseau, H. Pascard, and F. Willaime, Science **278**, 653 (1997).
[8] R. Tenne, L. Margulis, M. Genut, and G. Hodes, Nature (London) **360**, 444 (1992).

[9] L. Margulis, G. Salitra, R. Tenne, and M. Talianker, Nature (London) **365**, 114 (1993).
[10] Y. Feldman, E. Wasserman, D. Srolovitz, and R. Tenne, Science **267**, 222 (1995).
[11] A. Rothschild, S. Cohen, and R. Tenne, Appl. Phys. Lett. **75**, 4025 (1999).
[12] S. Cohen, Y. Feldman, H. Cohen, and R. Tenne, Appl. Surf. Sci. **145**, 603 (1999).
[13] M. Remskar, A. Mrzel, Z. Skraba, A. Jesih, M. Ceh, J. Demšar, P. Stadelmann, F. Lévy, and D. Mihailovic, Science **292**, 479 (2001).
[14] G. Seifert, H. Terrones, M. Terrones, G. Jungnickel, and T. Frauenheim, Phys. Rev. Lett. **85**, 146 (2000).
[15] R. Saito, G. Dresselhaus, and M. Dresselhaus, *Physical Properties of Carbon Nanotubes* (Imperial College Press, London, 1998).
[16] J. Perdew, K. Burke, and M. Ernzerhof, Phys. Rev. Lett. **77**, 3865 (1996).
[17] X. Gonze, J.-M. Beuken, R. Caracas, F. Detraux, M. Fuchs, G.-M. Rignanese, L. Sindic, M. Verstraete, G. Zerah, F. Jollet, M. Torrent, A. Roy, M. Mikami, Ph. Ghosez, T.-Y. Raty, and D.C. Allan, Comput. Mater. Sci. **25**, 478 (2002), note: ABINIT is a common project of the Université Catholique de Louvain, Corning Incorporated, and other contributors (http://www.pcpm.ucl.ac.be/ABINIT).
[18] L. Kleinman and D. Bylander, Phys. Rev. Lett. **48**, 1425 (1982).
[19] N. Troullier and J. Martins, Phys. Rev. B **43**, 1993 (1991).
[20] C. Broyden, Math. Comput. **19**, 577 (1965).
[21] N. Marzari, Ph.D. thesis, University of Cambridge, 1996.
[22] N. Marzari, D. Vanderbilt, A. De Vita, and M. Payne, Phys. Rev. Lett. **82**, 3296 (1999).
[23] M. Côté, M.L. Cohen, and D. Chadi, Phys. Rev. B **58**, R4277 (1998).
[24] X. Rocquefelte, F. Boucher, P. Gressier, G. Ouvrard, P. Blaha, and K. Schwarz, Phys. Rev. B **62**, 2397 (2000).
[25] A. F. Cotton, G. Wilkinson, C. A. Murillo, and M. Bochmann, *Advanced Inorganic Chemistry*, 6th ed. (Wiley, New York, 1999).
[26] D. Mihailovic (private communication).
[27] W.K. Hsu, B.H. Chang, Y.Q. Zhu, W.Q. Han, H. Terrones, M. Terrones, N. Grobert, A.K. Cheetham, H.W. Kroto, and D.R. Walton, J. Am. Chem. Soc. **122**, 10 155 (2000).
[28] P. Lambin, V. Meunier, L. Henrard, and A. Lucas, Carbon **38**, 1713 (2000).
[29] J. Colomer, L. Henrard, P. Lambin, and G. Van Tendeloo, Phys. Rev. B **64**, 125425 (2001).